

Setting the Operating Reserve Using Probabilistic Wind Power Forecasts

Manuel A. Matos, *Member, IEEE*, and R. J. Bessa

Abstract—In power systems with a large integration of wind power, setting the adequate operating reserve levels is one of the main concerns of system operators (SO). The integration of large shares of wind generation in power systems led to the development of new forecasting methodologies, including probabilistic forecasting tools, but management tools able to use those forecasts to help making operational decisions are still needed. In this paper, a risk evaluation perspective is used, showing that it is possible to describe the consequences of each possible reserve level through a set of risk indices useful for decision making. The new reserve management tool (RMT) described in the paper is intended to support the SO in defining the operating reserve needs for the daily and intraday markets. Decision strategies like setting an acceptable risk level or finding a compromise between economic issues and the risk of loss of load are explored. An illustrative example based on the Portuguese power system demonstrates the usefulness and efficiency of the tool.

Index Terms—Multicriteria decision, operating reserve, operating risk, uncertainty, wind power forecast.

I. INTRODUCTION

THE benefit of accurate wind power forecasting to power systems management is being increasingly recognized and became an important issue in defining the operation planning policies to be adopted by a system operator (SO), namely in accepting high wind penetration [1]. Currently, increasing the value of wind generation through the improvement of prediction systems' performance with new algorithms is one of the priorities in wind power forecasting [2], [3].

However, even the best tools are unable to eliminate the uncertainty associated to each particular forecast. The combination of generation and consumption variability and high uncertainty of forecasts can make it more difficult to fit wind generation into conventional procedures for power system operations, such as setting reserve levels or scheduling. Therefore, a correct management of the power system must take into account the uncertainties when making decisions.

Manuscript received August 01, 2009; revised February 03, 2010 and June 25, 2010; accepted August 03, 2010. Date of publication September 07, 2010; date of current version April 22, 2011. This work was performed in the framework of the project ANEMOS.plus (contract no 038692) funded in part by the European Commission under the 6th RTD Framework Programme. The work of R. J. Bessa was supported by Fundação para a Ciência e Tecnologia (FCT) Ph.D. Scholarship SFRH/BD/33738/2009. Paper no. TPWRS-00599-2009.

The authors are with the Instituto de Engenharia de Sistemas e Computadores do Porto (INESC Porto), Faculty of Engineering, University of Porto, Porto, Portugal (e-mail: mam@fe.up.pt; rbessa@inescporto.pt).

Color versions of one or more of the figures in this paper are available online at <http://ieeexplore.ieee.org>.

Digital Object Identifier 10.1109/TPWRS.2010.2065818

The integration of large shares of wind generation requires an increase in the amount of reserves that are needed to balance generation and load. Studies described in [4] showed that large scale integration of wind generation does not create problems in terms of primary reserve levels. So, the analysis should only be considered in terms of the operating reserve management.

The methods employed by the SO to define operating reserve requirements are generally deterministic, as can be seen in the survey presented in [5] about reserve categorization that reviews the criteria used across eight electrical systems. Sometimes, the UCTE rule [6] for defining secondary reserve is used as a reference for deterministic criteria. The rule depends only on the size of the typical load variations and is insensitive to the level of wind power of the system.

In a market environment, where the reserve cost will be part of the tariff paid by all customers, a trade-off between cost and risk should be considered instead of avoiding risk at almost any cost. On the other hand, since deterministic approaches do not in fact measure the risk, it may happen that, in some circumstances, complex risky situations are not covered. Therefore an approach based on deterministic criteria may lead, either to higher operational cost, or to excessive risk.

However, SO are starting to abandon deterministic rules, e.g., ERCOT (Texas Independent System Operator) already considers a probabilistic method for defining their monthly nonspinning reserve requirements [7]. The approach consists in setting a nonspinning reserve corresponding to percentile 95 of the historical total forecast error.

Probabilistic methods to address reserve assessment problems are well established in the literature (e.g., [8] and [9]), including the use of a risk threshold as a means to set the reserve [10]. Therefore, we will give more emphasis here to recent research that accounts for wind power forecast uncertainty. Strbac *et al.* [11] calculate the standard deviation of the combined wind and load uncertainty as that of the sum of the two independent Gaussian random variables. The reserve is defined to cover all variations contained within 3σ of the total system forecasting error, which means that 99.74% of variations are covered. The same approach is used by Holttinen [12], where the main goal was to estimate the increase in hourly load-following reserve requirements based on wind power generation and hourly load data in the four Nordic countries. Doherty *et al.* [13] present a methodology that relates the reserve level on the system in each hour to the number of load shedding incidents tolerated per year. Load and wind power forecast errors are incorporated in the model as Gaussian errors. All these approaches assume that the wind power forecast uncertainty may be represented by a Gaussian distribution. However, wind power forecast error is well known to have a non-Gaussian distribution [14]–[16]. An

alternative approach is not assuming any distribution for the uncertainty. Pahlow *et al.* [17] study the impact in load curtailment and reserve cost of several criteria based on the use of wind power ensembles that give a representation of the wind power forecast uncertainty. Kristoffersen *et al.* [18] describe a method adapted from the Wilmar Planning Tool where the wind power forecast uncertainty is modeled by discrete scenarios of day-ahead wind power generation generated by a method described in [19]. The power balance of each scenario is computed, and then it is assumed that a certain percentile of the total forecast error has to be covered by the reserve. Maurer *et al.* [20] compute the control area power imbalance distribution by convolving the distributions of generation and load. However, the authors do not clarify how the distributions are estimated or represented. The reserve is computed by setting a probability threshold for upward and downward reserve.

Nevertheless, most methods compute the reserve requirements associated with a reference risk level defined *a priori*. As stated above, a trade-off between cost and risk could instead be considered. Leite da Silva *et al.* [21] describe a methodology for evaluating the operating reserve requirements in a deregulated electrical market. They use system interruption costs, represented by loss of load cost (LOLC), and the reserve bid prices to balance risk and cost. Wang *et al.* [22] compute the optimal reserve capacity in the operating reserve market by minimizing the social cost, defined as the sum of the reserve cost with the expected cost of interruptions, represented by the interrupted energy assessment rates (IEAR). Ortega-Vazquez *et al.* [23] balance the spinning reserve cost and benefit in an electrical market with unit commitment. The benefit is a function of the reduction in the expected energy not supplied (EENS), and converted into socioeconomic cost by using the value of lost load (VOLL). Ortega-Vazquez *et al.* [24] extend their approach to include wind power forecast uncertainty, although the uncertainties are represented by Gaussian distributions and combined using the rule described in [11]. Morales *et al.* [25] describe a two-stage stochastic programming problem to compute the optimal reserve level and the cost of providing such reserve. The objective is to minimize the expected cost, considering the value of lost load and energy, as well as the reserve bids. Wind generation uncertainty is modeled through a set of scenarios, but no details are given about the scenarios generation method.

This paper presents a new reserve management tool (RMT) intended to support the SO in defining the reserve needs for the daily and intraday markets. Based on probabilistic wind power and load forecasts, risk indices are calculated that give information to the SO about the consequences of setting each possible reserve level. After interaction with the SO, the tool outputs the reserve levels to be set for the next day (or current day) that either: 1) enforce a maximum acceptable risk level; or 2) respect a trade-off limit between risk and reserve cost.

The structure of this paper is as follows: Section II presents the problem and the general methodology. In Section III, the details of the probabilistic model that computes the system generation margin distribution are described. Decision-making issues are discussed in Section IV. The management tool is demonstrated through an illustrative example in Section V. Section VI presents the conclusions.

II. GENERAL METHODOLOGY

The proposed tool addresses the problem of defining the operating reserve needs in a market environment where the SO acquires all of the reserve needed for the control area [26]. The allocation of reserve to each agent results from an auction mechanism where network constraints are not considered and reserve bids are made in an hour by hour basis. Therefore, ramp rates and other inter-temporal aspects would be mainly a concern of the bidders when preparing their offers.

Note that, the methodology can be applied or extended to other balancing mechanisms without any special difficulty.

A. Operation

In the daily market the SO at day D is in charge of defining the hourly reserve needs for the next day (day $D + 1$). The exercise starts from the feasible daily schedule that results from market clearing after congestion management analysis performed by the SO. Then, the SO, at time instant t_m , determines and publishes the reserve needs for each look-ahead time step of day $D + 1$, the time gap between the beginning of day $D + 1$ and the decision instant being equal to $24 - t_m$. These reserve amounts should then be split into secondary and tertiary reserves according to SO operating rules (problem not addressed in this paper).

The relevant inputs are the following variables: total load and wind power probabilistic forecasts, issued at time instant t_0 for each look-ahead time step of day $D + 1$, (time gap between the beginning of day $D + 1$ and the forecast instant equal to $24 - t_0$); daily generation schedule at time instant t_m for each look-ahead time step of day $D + 1$; failure rates of the conventional generation; interchange power levels.

Also in each intraday market session the SO has to define the reserve needs for the next day or for the remaining hours of the current day. The same framework may be used, the input data being “refreshed” with the new forecasts and with the feasible schedule decided by the intraday market.

B. Methodology

The approach computes first the probability distribution of the system total generation (G), for each look-ahead time step, by integrating the conventional generation unavailability distribution (C) and wind generation forecast uncertainty (W). Then, the system generation margin probability distribution (M), defined as the difference between total generation and load (L), is computed, taking into account the load forecast uncertainty.

For a specific level of operating reserve R (with its inherent cost), the distribution of $M + R$ can be used to calculate the loss of load probability (LOLP) and other reliability indices. This process is repeated for various values of R . As a result, curves with risk as a function of reserve (or its cost) can be obtained.

The aim here would be to minimize simultaneously risk and cost, which is not possible, due to the conflict between the two minimizations. Fig. 1 shows the complete structure of the tool.

In the second step of the methodology, the decision problem is formulated in a way suitable to incorporate the preferences of the decision maker (in this case the SO), and the final level of reserve is decided. So, the decision-aid model incorporates the

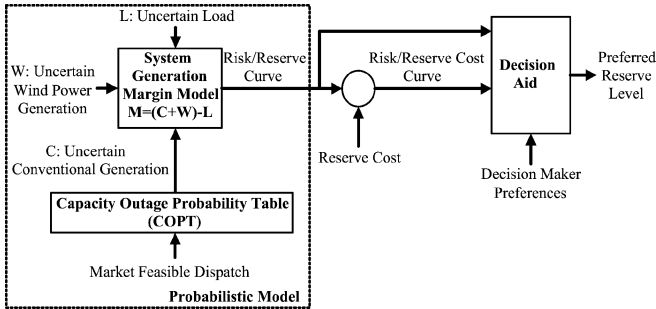


Fig. 1. Reserve management tool structure.

decision maker's preferences to help finding a preferred solution for each look-ahead time step.

III. PROBABILISTIC MODEL

A. Representation of Uncertainties

1) *Load*: Load forecast uncertainty is modeled through a Gaussian distribution with a given standard deviation and zero mean [9], approximated by a set of quantiles with 1% increment in nominal proportion from one quantile to the next.

Note that no changes are necessary in the methodology if the forecast uncertainty has a nonparametric representation (e.g., set of quantiles).

2) *Conventional Generation*: The probability mass function (*pmf*) of the conventional generation is analogous to the discrete probability distribution of the possible capacity states, usually known as the capacity outage probability table (COPT) [9]. Note that, because the subject is operating reserve, the outage replacement rate (ORR) is used instead of the forced outage rate (FOR) [9].

The method used in this paper to build the COPT is similar to the one described in [27], which is based on the fast Fourier transform (FFT) algorithm [28]. The method is computationally and mathematically attractive, since the computational time grows linearly with the number of machines in the system and can also accurately compute the COPT for systems with small ORR (which is the case, as the probabilities of failure during the lead time are very low).

The approach followed for the conventional generation consists in building a COPT using as input the conventional generation dispatched by the market clearing procedure and modified in order to guarantee a secure operation of the power system (frequently called feasible dispatch).

3) *Wind Generation*: Two sources of uncertainty in wind power are taken into account by the model, one coming from the forecast error and the other from possible wind turbines' unplanned outages.

The first source of uncertainty is related with the impossibility of producing perfect wind power forecast. Research work has been developed to estimate uncertainties in wind power forecast. As a result from the ANEMOS project, different methods to estimate the uncertainty of deterministic (or point) forecasts were developed [29].

The uncertainty of the deterministic forecast can be approached by different representations. The most common

representation is a nonparametric probabilistic forecast [14] represented by quantiles, intervals or probability density functions. The other two representations take the form of risk indices [14] of the forecasts, and scenarios incorporating temporal [30] or spatial [31] interdependence structure of prediction errors.

In this paper a nonparametric probabilistic forecast represented by a set of quantiles ranging from 5% to 95% with a 5% increment was used. Thus, and since the full probability distribution is required for convolution purposes, it is necessary to model the distribution's tails with exponential functions reflecting improbable extreme events [30].

The second source of uncertainty is related with the possible outages of the wind turbines and could be addressed in a way similar of the one used for the conventional generation. However, since there is a large number of a similar wind turbine (similar size and failure rate λ) a simpler model can be used. For instance, for a system with 2000 similar wind turbines, a failure rate of 10 failures/year, and a lead time of 24 h, the mean power (μ) is 97.26% of the rated power and the probability of having at least 96% of the rated power is 99.995% ($\mu - 4\sigma$). Therefore, an adjustment in the forecasted values using the mean value of the COPT (0.9726 in this case) is sufficient to capture the effect of wind turbines' outages.

B. System Generation Margin Model

The system generation margin is the amount that the available generating capacity exceeds the system load, so, being a function of two random variables (load and generation), it is also a random variable. In order to compute the system generation margin distribution (M), the inputs are the probability distributions of load (L), conventional generation (C) and wind power generation (W).

The first step is to compute the *pmf* of the sum of wind and conventional generation ($G = W + C$) for each look-ahead time step. Assuming independence, the sum can be computed by convolution [32]:

$$P_G(W + C = z) = \sum_{k=-\infty}^{\infty} P_W(W = z - k) \cdot P_C(C = k). \quad (1)$$

Finally, the system generation margin (M) is the difference between generation (G) and load (L), which requires also a convolution:

$$P_M(G - L = z) = \sum_{k=-\infty}^{\infty} P_G(G = z + k) \cdot P_L(L = k). \quad (2)$$

The preceding convolutions assume independence between load and wind power forecast uncertainties. Note that this has nothing to do with the possible correlation of wind power and load as a function of time.

The system generation margin distribution is a discrete probability distribution for each look-ahead time step, represented by its *pmf*, as depicted in Fig. 2.

The distribution can be calculated by just using (1) and (2) directly, but we used a more efficient way by making the computation in the frequency domain with the FFT method adapted from the one described in [33].

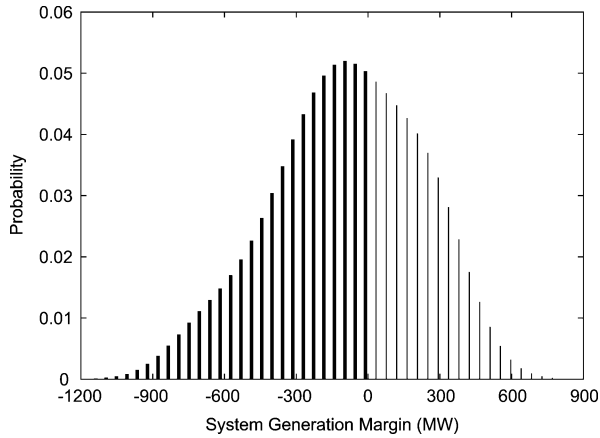


Fig. 2. pmf of the generation margin for a specific look-ahead time step.

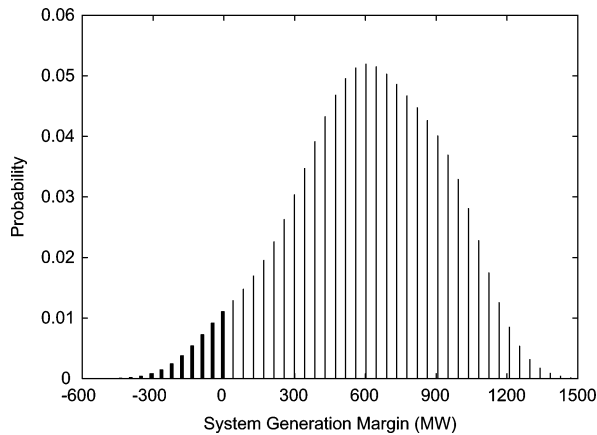


Fig. 3. pmf of the generation margin for an operating reserve of 700 MW.

Now, after setting a value for the operating reserve, the translation of the margin distribution ($M + R$) can be used to calculate the probability of losing load and other risk indices. Fig. 3 shows the effect of setting a reserve level of 700 MW in the same situation of Fig. 2. This additional capacity (as reserve) means shifting the Fig. 2 pmf to the right by the amount of the reserve 700 MW.

At this point, different risk related attributes meaningful for the decision maker can be computed. Following the approach described in [34], the idea is to extract risk attributes from the system generation margin distribution in order to give information about the impact of a potential reserve level.

The classical measures in reliability can be calculated from the system generation margin distribution, e.g., LOLP, loss of load expectation (LOLE), or EENS [9]. For instance, in the situation depicted in Fig. 2 (without any reserve), the risk would be described by $LOLP = 0.60$ and $EENS = 178.64$ MWh, but, after adding the 700-MW reserve, EENS reduces to only 4.13 MWh and LOLP to 0.04.

A direct reading of some risk attributes (LOLP, LOLE) is possible by taking the cumulative distribution of the negative margin. More elaborated indices (EENS) just require some statistical manipulation.

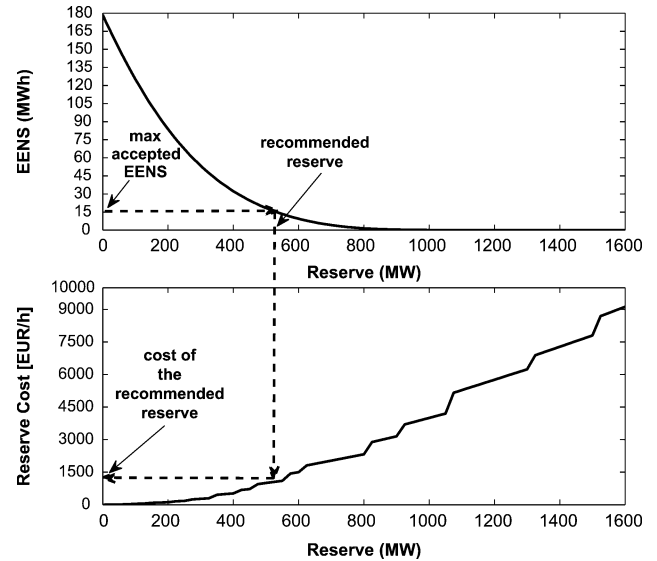


Fig. 4. Reserve that corresponds to the reference 15 MWh of EENS for a specific look-ahead time step.

Finally, note that other measures of risk, such as the conditional expected value of loss of load (XLLOL), value-at-risk or conditional value-at-risk [35] could be computed.

Risk measures (related with the downward reserve) can also be computed from the positive part of the system generation margin distribution. These risk measures are analogous to the ones related with the loss of load, for example: 1) probability of wasting renewable energy; 2) expected wasted renewable energy.

C. Reserve Cost

The cost of buying reserve in the market can be assessed by a curve representing the bids offered by the market agents for selling upward and downward reserve. The bids for selling reserve are paid at the bid price or by the marginal price [36]. A typical curve of the reserve cost for the former case can be seen in the bottom of Fig. 4.

IV. DECISION-MAKING ISSUES

The preceding analyses and results are the mathematical basis to set the level of operating reserve, since they allow the operator to evaluate the risk associated to a specific level of reserve.

However, it is convenient to formalize a decision making phase where the decision maker communicates preferences and makes the final decision, sometimes introducing explicitly economic aspects. In this section, three alternative methods for decision-making are described.

A. Setting a Threshold for a Risk Attribute

The simplest approach consists in setting a threshold value for the maximum acceptable risk. If the proposed reserve level leads to excessive risk then the reserve level must be increased until the actual risk value is lower than the threshold. Of course, the

reserve needs for a specific threshold can be read immediately if a risk/reserve curve was previously constructed.

For instance, in Fig. 4, in order to assure an EENS not greater than 15 MWh, a reserve level of at least 530 MW would be necessary.

In this case, the decision maker does not take into account the reserve cost, (although it is possible to calculate it, 1200€, in the example) so it may happen that expensive additional capacity is needed to maintain the risk below the threshold.

B. Multicriteria Approach

If, instead of just setting a threshold, the decision maker wants to balance risk and cost, a multicriteria approach can be used to help. Two possibilities were considered, one based on trade-offs for direct compensation between attributes, the other modeling more complex preference structures with nonlinear value functions.

1) *Equivalent Cost Approach*: The equivalent cost approach uses a constant trade-off between reserve cost and an associated risk measure (e.g., EENS). The trade-off μ ($= \Delta C / \Delta R$) is the rate at which the decision maker is ready to give up ΔC units of cost in exchange for gaining ΔR units in the risk criterion, while remaining indifferent between the two solutions [37]. For example, if the two criteria are EENS and cost, the trade-off can be interpreted as how much the decision maker is willing to pay to decrease the EENS, and would be expressed in €/MWh.

In this approach, after eliciting the trade-off μ from the decision maker, we just need to find the reserve level r that minimizes the equivalent cost $EqCost(r) = Cost(r) + \mu \cdot Risk(r)$. Sensitivity analysis around μ may help the decision maker choosing the best final value of the reserve.

Some authors, such as [22]–[24], assume that the value of μ is equal to the cost of energy not supplied, e.g., VOLL. This may of course be a point of departure when setting the trade-off, but the final value of μ should also reflect the risk attitude of the decision maker.

2) *Value Function Approach*: In order to capture more complex preference structures than the ones behind a constant trade-off, nonlinear value functions can be used. We will restrict the approach to additive value functions [38], but more complex functions could be used.

The approach consists in building an individual value function for each criterion, and then assessing weights to build the multi-attribute value function whose maximization leads to the preferred reserve level r . Note that, if the individual value functions are all linear, the model reduces to the trade-off approach.

A possible multi-attribute value function for this problem would be

$$v_{Cost,EENS}(r) = k_{Cost} \cdot v_{Cost}(Cost(r)) + k_{EENS} \cdot v_{EENS}(EENS(r)) \quad (3)$$

where v_{Cost} and v_{EENS} are the individual value functions for the two criteria and k_{EENS} and k_{Cost} are parameters, usually know as weights ($k_{Cost} + k_{EENS} = 1$).

The shape of the individual value functions reflects the variation of the decision maker's increase (decrease) of satisfaction along the corresponding attribute. The individual value function

TABLE I
CONVENTIONAL GENERATION DATA

Type	Rated Power (%)	Number of Units
<i>Hydro</i>	4576.2	93
<i>Fuel-oil</i>	1712.6	12
<i>Coal</i>	1776	6
<i>Combine Cycle</i>	2166	6
<i>Diesel</i>	165	2

of the cost is usually linear, because the increase in decision maker satisfaction for a specific cost saving is generally independent of the cost level. On the other hand, one may see different attitudes regarding EENS: 1) A decision maker may be very favorable to the decrease of the EENS when its level is high, but not so enthusiastic when the EENS level is already acceptable or low; 2) Another decision maker, in contrast, could intensify the willingness to pay for reducing risk when approaching the best (lower) levels of EENS. Neither of these attitudes can be classified as correct or incorrect—they simply correspond to different managing styles and external constraints influence.

In order to capture the decision maker attitude regarding risk (in this case through EENS), an exponential value function is proposed, due to its flexibility:

$$v_{EENS}(r) = \frac{e^{b \cdot z(r)} - 1}{e^b - 1} \quad (4)$$

where $z(r) = \frac{(EENS^{\max} - EENS(r))}{(EENS^{\max} - EENS^{\min})}$.

In fact, by changing parameter b it is possible to change the underlying preference structure. Negative values of b reflect attitude 1) described earlier, while positive values of b correspond to attitude 2).

The last step consists in determining the weights k_{Cost} and k_{EENS} , using the following procedure:

- 1) Get an indifference judgment from the decision maker. For instance, the decision maker states indifference between solutions A and B ($A \sim B$).
- 2) Use the information $A \sim B$ to set $v_{Cost,EENS}(A) = v_{Cost,EENS}(B)$ and, in conjunction with $k_{Cost} + k_{EENS} = 1$, compute the weights.

It is important to point out that it is always possible to obtain the indifference judgment by starting with two relatively arbitrary alternatives and making changes in one of them (increase risk, decrease cost, etc.) until the indifference is reached. More details about this kind of procedure can be seen in [37] or [38].

V. ILLUSTRATIVE EXAMPLE

A. Description

The example used to illustrate the methodology is a single bus model based on the Portuguese power system. The total installed capacity of conventional generation is 10395.8 MW and the system has 2742 MW of wind power capacity.

The system has 119 units of conventional generation divided as shown in Table I.

The lead time considered to compute the ORR of each unit is one hour. The forecasted load curve for the 24-h period of a

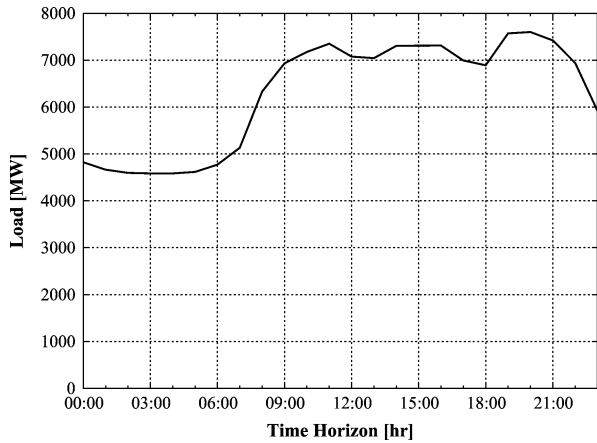


Fig. 5. Forecasted load for a 24-h period.

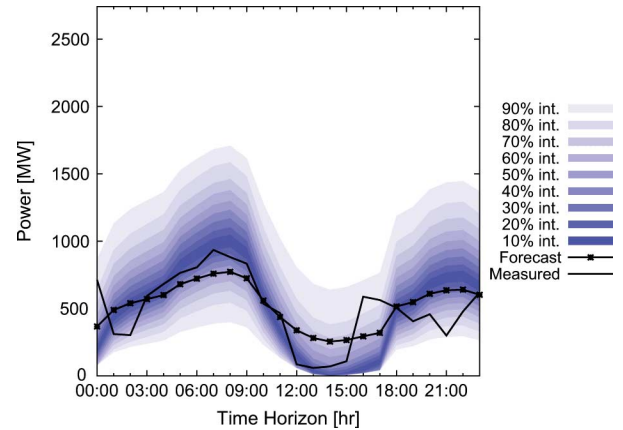


Fig. 7. Point forecast and a set of interval forecasts for scenario L.

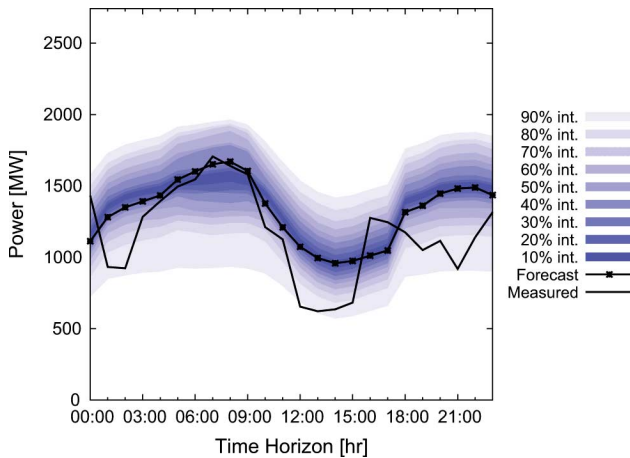


Fig. 6. Point forecast and a set of interval forecasts for scenario H.

weekday is shown in Fig. 5, where the peak load was 7600 MW at 20:00.

The load forecast uncertainty is modeled through a Gaussian distribution with standard deviation computed from a typical mean absolute percentage error (MAPE) of 2% [26] (note that $\sigma = 1.4826$ MAPE).

For illustrative purposes, we chose a day with a typical pattern of the wind generation behavior in Portugal, and used global system wind power forecasts and uncertainty similar to the ones produced by the ANEMOS platform.

Although it is beyond the scope of the present paper, we must stress that the quality of probabilistic forecasts should be evaluated (a possible framework is proposed in [39]).

In Figs. 6 and 7, a forecasted distribution for each hour, represented by 19 percentiles, is depicted for scenarios with high wind generation (scenario H) and low wind generation (scenario L).

Since in Portugal wind energy receives a feed-in tariff and does not go to the market, the market load (conventional generation) is the difference between the point forecast of the wind generation and the load forecast. In this test, the reserve needs are estimated by the SO for the next day in the daily market session of the MIBEL market.

We will now apply the methodology to the case study. The first step is the determination of the risk/reserve and risk/reserve cost curves (shown later in Figs. 11 and 13), as a basis to the application of the different decision making procedures described in Section IV. However, for comparison, the following rules will be also considered:

Rule A) Secondary reserve given by the UCTE rule ($\sqrt{10 \cdot L_{\max} + 150^2} - 150$, L_{\max} being the peak load); tertiary reserve covers the loss of the largest generating unit [6].

Rule B) Secondary reserve equal to $6 \cdot \sqrt{L}$ (L is the forecast hourly load) when the load variation is fast and $3 \cdot \sqrt{L}$ otherwise, tertiary reserve is computed hourly as the rated power of the largest unit within the system plus 2% of the forecast hourly load; rule used in Spain [26].

Rule C) Based on the probabilistic rule described in [11]. The operating reserve is given by $\varepsilon \cdot \sqrt{\sigma_L^2 + \sigma_W^2 + \sigma_C^2}$, where ε is a parameter related with the desired confidence level (e.g., $\varepsilon = 3$ means that 99.74% of variations are covered) and σ is the standard deviation of wind generation (W), load (L) and conventional generation (C). The three distributions are assumed to be Gaussian; σ_W was computed directly from the forecasted uncertainty and σ_C from the COPT.

B. Risk/Reserve Based Decisions

We first simulated a situation where a threshold for the LOLE was previously set by the decision maker. In this case, the reserve level can be obtained directly from the risk/reserve curve. In Fig. 8 a comparison is depicted between the reserve needs obtained using our tool (RMT) and rule C for scenario H. The contribution of combined conventional generation and load uncertainty for the reserve needs is identified (with wind generation deterministic forecast). The threshold for the LOLE was defined by the decision maker as 1 min/h (which corresponds to $\varepsilon = 2.13$, in rule C).

The shape of the reserve needs curve obtained with a deterministic forecast for wind power (“no wind power uncertainty” in Fig. 8) is similar to the load shape. As expected, integration of wind generation uncertainty in the model leads to an increase in the reserve requirements.

For the same threshold level, Fig. 9 shows a comparison between the RMT and rules A, B, and C.

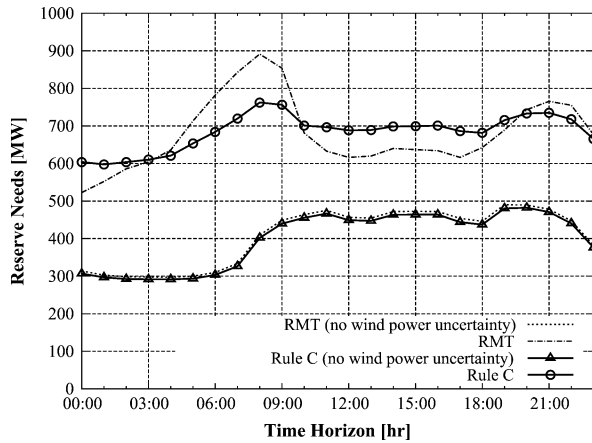


Fig. 8. Reserve needs with and without wind generation uncertainty using the RMT and rule C.

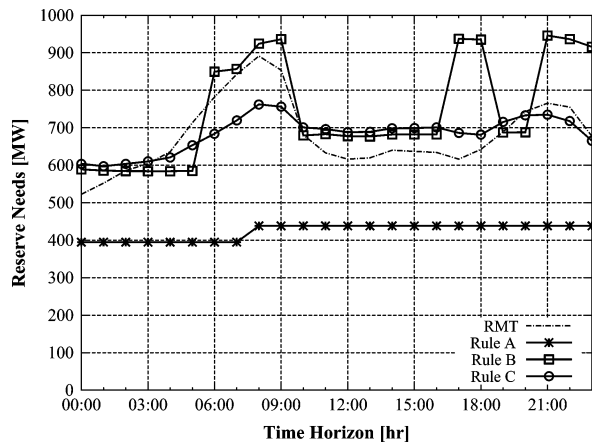


Fig. 9. Reserve needs obtained using RMT and rules A, B, and C.

The reserve needs obtained with rule A have almost the same value all day, the only variation being due to the capacity of the largest unit. On the other hand, Rule B seems to ask for additional reserve in order to deal with the wind generation variability. Applying rules A and B does not provide the SO information about the risk taken, and both are insensitive to wind power level.

Rule C allows the definition of the acceptable level of risk. The reserve needs without wind power forecast uncertainty are almost equal to the ones obtained with the RMT. The difference becomes significant when the wind power forecast uncertainty is added; in this case, the results differ significantly. This is due to the Gaussian assumption for wind power forecast uncertainty incorporated in rule C, which is not confirmed.

In order to analyze the quality of each suggested reserve level a Monte Carlo simulation was performed for hour 8:00. The quality criterion is the number of loss of load occurrences in a simulation with 20 000 random samples taken from the forecasted distributions of each variable. The results are presented in Table II.

The result obtained with the RMT is consistent with the risk threshold defined. Rule C presents a LOLE value higher than the max accepted level. The assumption of a Gaussian distribution for wind power forecast uncertainty is not adequate, so the real

TABLE II
RESULTS OF THE MONTE CARLO SIMULATION FOR HOUR 8:00

	Loss of load occurrences (%)	min/hour
<i>RMT</i>	1.37	0.82
<i>Rule A</i>	19.21	11.52
<i>Rule B</i>	1.07	0.64
<i>Rule C</i>	6.60	3.96

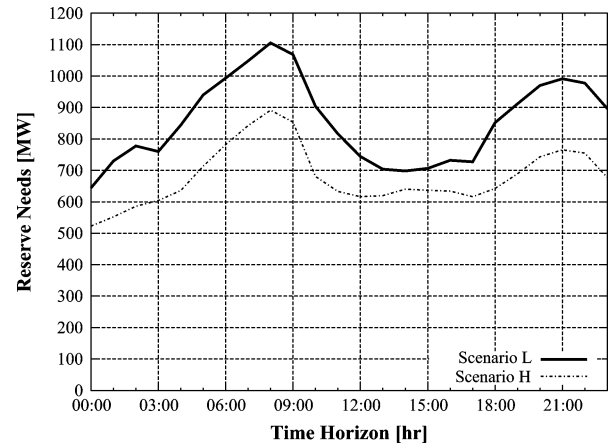


Fig. 10. Reserve needs of scenarios H and L.

risk is most of the times higher than stipulated (although the inverse may also occur). This happens because the skewness of the error distribution is generally positive (see [15, Ch. 4]) and therefore the density of the distribution is concentrated on the over-prediction part.

Taking into account the stipulated risk, Rule A conducts to excessive risk and Rule B leads to an excessive reserve level. Variation of the stipulated risk could change these situations, but, since the rules are deterministic, only by chance they could satisfy the threshold.

As shown in Fig. 10, although wind generation in scenario L is lower than scenario H, the reserve needs for scenario L are higher when compared with the ones obtained for H. This result illustrates that it is not only the level of wind generation which has impact on reserve needs, but also the amount of wind generation uncertainty and the shape of its distribution. Scenario L presents a higher amount of wind power forecast uncertainty, since the inter-quantile range of this scenario is higher.

However, a closer look at hour 8:00 in Figs. 6 and 7 shows that a higher reserve for scenario H was expected since the probability of having wind generation below the point forecast (value used to compute the conventional generation needs) is greater than in scenario L. This is true for the initial system generation margin. However, as depicted in the risk/reserve curves of Fig. 11, there is an intersection of the two scenarios' curves. If the decision maker chooses a reference LOLE of 20 min/h then the reserve will be higher in scenario H, but if the LOLE is 10 min/h the reserve will be higher in scenario L. This behavior is due to the shape of the wind power forecast uncertainty, which is reflected in the system generation margin. As depicted in Fig. 12 for a reserve of 200 MW, the sum of the probabilities of the negative distribution for scenario H is higher, but when the level of

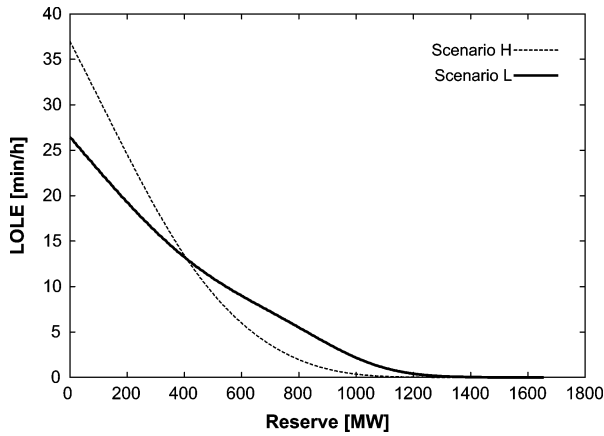


Fig. 11. Risk/reserve curve for hour 8:00 of scenarios H and L.

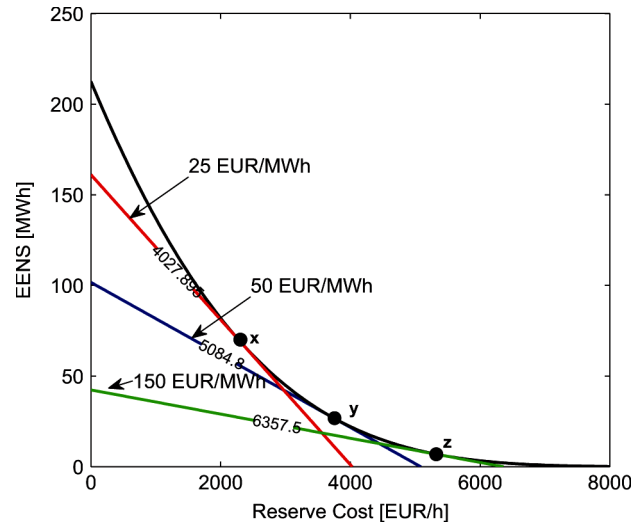


Fig. 13. Indifference lines of the constant tradeoffs ($\mu = 25, 50$ and 150 €/MWh).

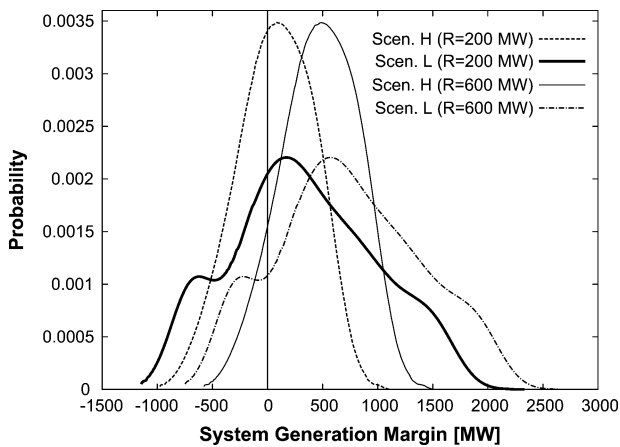


Fig. 12. Generation margin pmf for hour 8:00 of scenarios H and L.

reserve increased to 600 MW, scenario L has a higher sum of probabilities of negative values than scenario H.

C. Risk/Cost Based Decisions

For simplicity, and without loss of generality, only look-ahead time 8:00 of scenario H is analyzed in this section.

Each equivalent cost function value defines a family of linear indifference lines (set of alternatives that are valued in the same way by the decision maker), which describes the preference structure of the decision maker and their slope is the reference trade-off value.

Fig. 13 shows the indifference lines for three reference trade-off values (25, 50 and 150 €/MWh) and the risk/cost of reserve curve. Each curve connects all points that are indifferent for the decision maker, since they have the same equivalent cost. For instance, for the trade-off 50 €/MW the preferred solution (y) is the one in the indifference line that has an equivalent cost of 5084.8€ and corresponds to a reserve of 512 MW, EENS = 27.2 MWh and reserve cost = 3724 €. Now, a different decision maker, more concerned with the level of EENS, sets a greater trade-off of 150 €/MW, and the preferred solution (z) will be different: more reserve (730 MW); less risk (EENS = 6.7 MWh) and higher cost (5352 €). Solution (x) represents a trade-off value of 25 €/MWh, and we see that the slope of the indifference curve changes according to

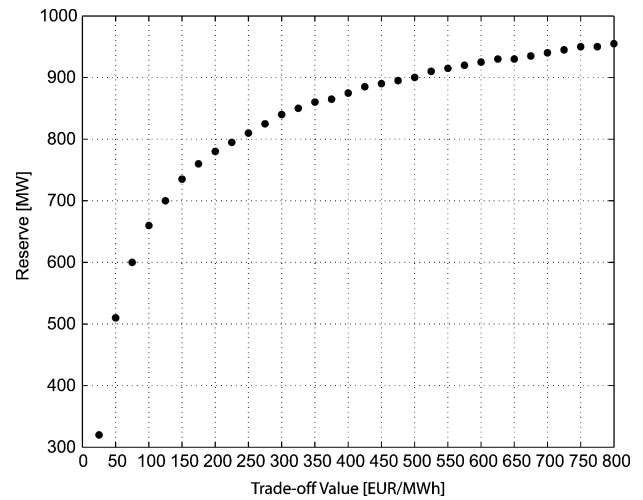


Fig. 14. Reserve requirements obtained with different trade-off values.

the preferences of the decision maker, moving the preferred solution along the risk/cost curve.

Fig. 14 depicts the reserve obtained using trade-off values ranging from 25 to 800 €/MWh. As expected, as the trade-off value changes, the preferred solution moves along the risk/cost of reserve curve. For lower trade-off values the preferred solutions are in the part of the risk/cost of reserve curve with higher slope and therefore variations of 25 €/MW in the trade-off lead to higher variations in the reserve (e.g., it increases 190 MW when the trade-off changes from 25 to 50 €/MWh). As we move to zones with lower slope, the difference between the solutions becomes smaller. For instance, for trade-offs between 350 and 550 €/MW the reserve only varies from 860 to 915 MW.

For more complex preference attitudes, a nonlinear value function can be used. For a decision maker indifferent between (5000,60) and (5500,50) and accepting an exponential function with $b = -4$ [see (4)] for the EENS valuation, the (nonlinear) indifference curves are depicted in Fig. 15.

Since the trade-off is not constant, in the area of high EENS, a small decrease in EENS offsets a large increase in reserve

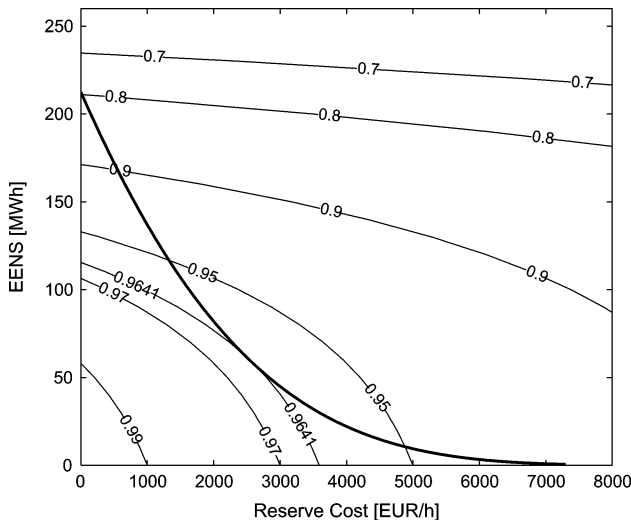


Fig. 15. Indifference curves of the exponential function with $b = -4$.

cost (the indifference curves are little sloped), because the decision-maker is prepared to pay the necessary to avoid high values of EENS. By contrast, in the low EENS, a big decrease in EENS offsets a small increase in reserve cost, since the values of EENS are tolerable, the decision maker will just pay something if a large decrease of EENS happens. In summary, the trade-off in the first area of the curve is very high, and in the second is very low. Of course, intermediate values of EENS conduct to intermediate values of the trade-off.

The preferred solution is in the indifference curve with value 0.9641 and corresponds to a reserve of 340 MW, EENS of 62.3 MWh and cost of 2474 €.

VI. CONCLUSIONS

This paper describes a methodology developed to support system operators in defining the operating reserve needs, taking into account conventional generation outages, load forecast uncertainty and wind power forecast uncertainty.

The methodology avoids making assumptions on the wind power forecast distribution, and instead uses probabilistic forecasts directly provided by the wind power forecast system. On the other hand, decisions are supported by a comprehensive quantification of risk through meaningful indices. The example shows, for illustration, realistic situations where this approach is more appropriate than applying rigid deterministic rules or Gaussian assumptions. Future work will use data now being collected for a long period of time to extend the evaluation.

Besides the risk/reserve curve computation, the methodology addresses decision making issues, namely when reserve cost and risk are to be included simultaneously in the decision process. The methodology is able to model different attitudes and values of the decision maker, as illustrated in the case study, in order to support a rational decision process.

This methodology can also support the decision maker in defining the operating reserve to deal with the risk of having surplus of generation during valley hours. The decision strategies are analogous to ones presented in this paper and the only

difference is in working with the positive part of the system generation margin distribution.

The tool is oriented for a deregulated electricity market. However, the methodology can easily be adapted to other reserve definition mechanisms or can be combined with a unit commitment procedure.

REFERENCES

- [1] M. L. Ahlstrom, L. Jones, R. Zavadil, and W. Grant, "The future of wind forecasting and utility operations," *IEEE Power Energy Mag.*, Special Issue: Working with Wind; Integrating Wind into the Power System, vol. 3, no. 6, pp. 57–64, Nov./Dec. 2005.
- [2] A. Costa, A. Crespo, J. Navarro, G. Lizcano, H. Madsen, and E. Feitosa, "A review on the young history of the wind power short-term prediction," *Renew. Sustain. Energy Rev.*, vol. 12, no. 6, pp. 1725–1744, Aug. 2008.
- [3] G. Giebel, R. Brownsword, and G. Kariniotakis, State of the Art on Short-Term Wind Power Prediction, 2003, ANEMOS Deliverable Report D1.1.
- [4] H. Banakar, C. Luo, and B. T. Ooi, "Impacts of wind power minute-to-minute variations on power system operation," *IEEE Trans. Power Syst.*, vol. 23, no. 1, pp. 150–160, Feb. 2008.
- [5] Y. Rebours and D. S. Kirschen, A Survey of Definitions and Specifications of Reserve Services, Univ. Manchester, Manchester, U.K., 2005.
- [6] UCTE Operating Handbook—Policies P1: Load-Frequency Control and Performance, 2004.
- [7] D. Maggio, "Integrating wind forecasting into market operation-ERCOT," in *Proc. Presentation at Utility Wind Integration Group (UWIG) Workshop*, Phoenix, AZ, Feb. 2009, pp. 18–19.
- [8] L. L. Garver, "Effective load carrying capability of generating units," *IEEE Trans. Power App. Syst.*, vol. PAS-85, pp. 910–919, Aug. 1966.
- [9] R. N. Allan and R. Billinton, *Reliability Evaluation of Power Systems*. New York: Plenum, 1984.
- [10] D. Chattopadhyay and R. Baldick, "Unit commitment with probabilistic reserve," in *Proc. IEEE Power Eng. Soc. Winter Meeting*, New York, 2002, vol. 1, pp. 280–285.
- [11] G. Strbac, A. Shakoob, M. Black, D. Pudjianto, and T. Boppe, "Impact of wind generation on the operation and development of the UK electricity systems," *Elect. Power Syst. Res.*, vol. 77, no. 9, pp. 1214–1227, Jul. 2007.
- [12] H. Holttinen, "Impact of hourly wind power variations on the system operation in the Nordic countries," *Wind Energy*, vol. 8, no. 2, pp. 197–218, 2004.
- [13] R. Doherty and M. O'Malley, "New approach to quantify reserve demand in systems with significant installed wind capacity," *IEEE Trans. Power Syst.*, vol. 20, no. 2, pp. 587–595, May 2005.
- [14] P. Pinson, "Estimation of the uncertainty in wind power forecasting," Ph.D. dissertation, Ecole des Mines de Paris, Paris, France, 2006.
- [15] N. Siebert, "Development of methods for regional wind power forecasting," Ph.D. dissertation, Ecole des Mines de Paris, Paris, France, 2008.
- [16] M. Lange, "On the uncertainty of wind power predictions—Analysis of the forecast accuracy and statistical distribution of errors," *J. Solar Energy Eng.—Trans. ASME*, vol. 127, no. 2, pp. 177–194, May 2005.
- [17] M. Pahlow, C. Möhrlein, and J. U. Jørgensen, "Application of cost functions for large scale integration of wind power using a multi-scheme ensemble prediction technique," in *Optimization Advances in Electric Power Systems*, E. D. Castronuovo, Ed. Commack, NY: Nova, 2009, ch. 7.
- [18] T. Kristoffersen, P. Meibom, J. Apfelbeck, R. Barth, and H. Brand, WP3 Prototype Development for Operational Planning Tool, 2008, Tech. Rep. Risø-R-1666.
- [19] L. Soder, "Simulation of wind speed forecast errors for operation planning of multiarea power systems," in *Proc. Int. Conf. Probabilistic Methods Applied to Power Systems (PMAPS 2004)*, Sep. 12–16, 2004, pp. 723–728.
- [20] C. Maurer, S. Krahl, and H. Webe, "Dimensioning of secondary and tertiary control reserve by probabilistic methods," *Eur. Trans. Elect. Power*, vol. 19, no. 4, pp. 544–552, Jan. 2009.
- [21] A. M. Leite Da Silva and G. P. Alvarez, "Operating reserve capacity requirements and pricing in deregulated markets using probabilistic techniques," *IET Gen., Transm., Distrib.*, vol. 1, no. 3, pp. 439–446, May 2007.

- [22] J. Wang, X. Wang, and Y. Wu, "Operating reserve model in the power market," *IEEE Trans. Power Syst.*, vol. 20, no. 1, pp. 223–229, Feb. 2005.
- [23] M. A. Ortega-Vazquez and D. S. Kirschen, "Optimizing the spinning reserve requirements using a cost/benefit analysis," *IEEE Trans. Power Syst.*, vol. 22, no. 1, pp. 24–33, Feb. 2007.
- [24] M. A. Ortega-Vazquez and D. S. Kirschen, "Estimating the spinning reserve requirements in systems with significant wind power generation penetration," *IEEE Trans. Power Syst.*, vol. 24, no. 1, pp. 114–124, Feb. 2009.
- [25] J. M. Morales, A. J. Conejo, and J. Perez-Ruiz, "Economic valuation of reserves in power systems with high penetration of wind power," *IEEE Trans. Power Syst.*, vol. 24, no. 2, pp. 900–910, May 2009.
- [26] E. L. Miguélez, I. E. Cortés, L. R. Rodríguez, and G. L. Camino, "An overview of ancillary services in Spain," *Elect. Power Syst. Res.*, vol. 78, no. 3, pp. 515–523, Mar. 2008.
- [27] R. N. Allan, A. M. Leite da Silva, A. Abu-Nasser, and R. C. Burchett, "Discrete convolution in power system reliability," *IEEE Trans. Reliab.*, vol. 30, pp. 452–456, 1981.
- [28] J. W. Cooley and J. W. Tukey, "An algorithm for the unit calculation of complex Fourier series," *Math. Comput.*, vol. 19, no. 90, pp. 297–301, 1965.
- [29] P. Pinson, H. A. Nielsen, H. Madsen, M. Lange, and G. Kariniotakis, Methods for the Estimation of the Uncertainty of Wind Power Forecasts, Informatics and Mathematical Modeling, Technical Univ. Denmark, 2007, ANEMOS project deliverable report D3.1b.
- [30] P. Pinson, G. Papaefthymiou, B. Klockl, H. A. Nielsen, and H. Madsen, "From probabilistic forecasts to statistical scenarios of short-term wind power production," *Wind Energy*, vol. 12, no. 1, pp. 51–62, 2009.
- [31] G. Papaefthymiou and P. Pinson, "Modeling of spatial dependence in wind power forecast uncertainty," in *Proce. 10th Int. Conf. Probabilistic Methods Applied to Power Systems (PMAPS 2008)*, Mayagüez, PR, May 2008.
- [32] R. C. Williamson, "Probabilistic arithmetic," Ph.D. dissertation, Univ. Queensland, Brisbane, Australia, 1990.
- [33] M. Kohl, P. Ruckdeschel, and T. Stabla, General Purpose Convolution Algorithm for Distributions in S4-Classes by Means of FFT, 2005.
- [34] M. A. Matos, "Decision under risk as a multicriteria problem," *Eur. J. Oper. Res.*, vol. 181, no. 3, pp. 1516–1529, Sep. 2007.
- [35] F. Wu, Y. Hou, and H. Zhou, "Measuring reliability (or risk) coherently," in *Proc. 16th Conf. Power Systems Computation (PSCC 2008)*, Glasgow, U.K., Jul. 14–18, 2008.
- [36] A. E. Kahn, P. C. Cramton, and R. H. Porter, "Uniform pricing or pay-as-bid pricing: A dilemma for California and beyond," *Elect. J.*, vol. 14, no. 6, pp. 70–79, 2001.
- [37] R. T. Clemen and T. Reilly, *Making Hard Decisions With Decision Tools*. Pacific Grove, CA: Duxbury, 2001.
- [38] R. Keeney and H. Raiffa, *Decision With Multiple Objectives: Preference and value Tradeoffs*. New York: Wiley, 1976.
- [39] P. Pinson, H. A. Nielsen, J. K. Møller, H. Madsen, and G. Kariniotakis, "Nonparametric probabilistic forecasts of wind power: Required properties and evaluation," *Wind Energy*, vol. 10, no. 6, pp. 497–516, 2007.

Manuel A. Matos (M'94) was born in 1955 in Porto, Portugal. He received the El. Eng., Ph.D., and Aggregation degrees.

He has been with the Faculty of Engineering of the University of Porto (FEUP) since 1978 (Full Professor since 2000). He is also coordinator of the Power Systems Unit of INESC Porto. His research interests include classical and fuzzy modeling of power systems, reliability, optimization, and decision-aid methods.

R. J. Bessa received the Licenciado (five-year) degree in electrical and computer engineering from the Faculty of Engineering of the University of Porto, Porto, Portugal (FEUP), in 2006 and the M.Sc. degree in data analysis and decision support systems from the Faculty of Economy of the University of Porto (FEP) in 2008. He is pursuing the Ph.D. degree in the Doctoral program in Sustainable Energy Systems (MIT Portugal) at FEUP.

Currently, he is a researcher at INESC Porto in its Power Systems Unit. His research interests include wind power forecasting, electric vehicles, data mining, and decision-aid methods.